Optimizing the Operational Parameters of an Electrochemical Purification Cell for Corrosion Mitigation in CSP Plants During Operation

Kerry Rippy, Elizabeth Howard, Liam Witteman, and Judith Vidal

National Renewable Energy Laboratory, Golden, Colorado (USA)

Abstract

To make concentrating solar power (CSP) cost-competitive, the next generation of CSP plants will increase efficiency by operating at a higher temperature, which will require a new thermal energy storage material. One option for the thermal energy storage material is a ternary chloride salt that is stable at the temperatures required, but reacts easily with the atmosphere to form MgOHCl, a corrosive impurity. If left unchecked, this impurity will corrode the containment alloys, potentially leading to dangerous spills. We are working to design an electrochemical purification cell to remove MgOHCl from the molten chloride salt during CSP plant operation. In this paper, we use specification of the Gen3 CSP liquid pathway pilot plant to assess the rate at which purification must occur. Additionally, we analyze possible process flow pathways integration of the purification cell into the pilot plant in order to achieve target purification rate. Ultimately, we determine that implementation of a single reactor through which all chloride salts flow is the most efficient design to reduce impurity concentration below 0.1 mol % impurity.

Keywords: Concentrating Solar Power, Chloride Salts, Corrosion Mitigation, Electrochemical Purification

1. Introduction

The U.S. Department of Energy's (DOE) SunShot Initiative includes cost and performance goals for concentrating solar power (CSP) systems (Mehos et al. 2017). CSP is an excellent candidate to replace nonrenewable energy sources because it stores thermal energy to generate electricity on demand. For CSP to meet the goals outlined by the SunShot Initiative, the next generation of CSP plants (Gen3) will need to operate at a higher temperature than the current heat transfer fluid will allow. DOE has supported the development of plans to use the ternary molten chloride salt NaCl-KCl-MgCl2 as the heat transfer fluid in the Gen3 CSP plants, because it is stable above 800°C and relatively inexpensive (Ding, Gomez-Vidal, et al. 2019; Ding, Shi, et al. 2019).

The primary barrier to using molten chloride salt in a CSP plant is that it is highly corrosive, especially at the high temperatures required (Ding, Gomez-Vidal, et al. 2019). Corrosion in molten chloride salt is driven by oxide and hydroxide impurities (Gomez-Vidal and Tirawat 2016). A procedure using particles of electropositive Mg can purify the salt prior to use in the CSP plant, but the ternary chloride salt is strongly hygroscopic, which leads to corrosive impurity formation during plant operation (Gomez-Vidal and Tirawat 2016). Specifically, any interaction of the molten chloride salt with water in the atmosphere leads to the formation of MgOHCl, which ionizes into corrosive $MgOH^+$. The Mg particle purification procedure cannot be used within the CSP plant, because it relies on temperatures above 650°C to melt the Mg particles, and the cold side of the next generation of CSP plant will be at 500°C (Mehos et al. 2017).

To remove impurities that enter the molten salt during CSP plant operation, we are designing an electrochemical cell with Mg anodes to reside in the cold side of the plant. The electrochemical system has been shown to control corrosion at the lab scale. We predicted the rate of moisture ingress into the CSP plant to provide an upper bound on the concentration of MgOH+ entering the purification cell. Then, we selected and modeled various salt flow pathways to identify ideal process flow.

doi:10.18086/solar.2021.01.01 Available at http://proceedings.ises.org

2. Results and Discussion

2.1. Specifications of the CSP Plants

The modeling in this paper uses the specifications of a conceptualized pilot plant, obtained from the CSP Gen3 Liquid-Phase Pathway to SunShot report.(Turchi et al. 2021)

The pilot plant will utilize a commercial ternary $MgCl_2$–KCl–NaCl salt. It will have a total salt inventory of 180 MT or 2.15 x 10^6 mol. Variation of the volumetric flow rate of molten salt through the pilot plant (Q) is expected. In this work, we use Q = 110 gpm as the default volumetric flow rate within the reactor. The purification cell will be located on the cold side of the plant, with a temperature of 500 °C.(Turchi et al. 2021)

A contiuous sweep of $N_2(g)$ is required to protect pump components from salt vapor deposition and freezing. The expected sweep rate in the pilot plant is approximately 15 scfm (24 Nm3 /h). In the high purity $N_2(g)$ will be used, up to 1 ppm H_2O may be present.

2.2. Formation of corrosive impurities in salt

According to Zhao et al.,(Zhao, Klammer, and Vidal 2019) when the corrosive species $MgOH^+$ is present in the ternary salt at 5 wt. %, the yearly corrosion rate of Haynes 230 is greater than 3200 µm per year. When the concentration of this species is reduced to less than 0.5 wt. %, the yearly corrosion rate of Haynes 230 is reduced to around 40 µm per year. Thus, it is essential to keep the concentration of $MgOH^+$ low.

However, MgOHCl forms within the ternary salt when exposed to moisture via reaction (1). Based on ongoing work, reaction (1) is fast; mass transport of water vapor through the diffusion boundary layer is the limiting step in this process. Given ullage gas residence times on the order of seconds or more, turbulent ullage gas flow, and high ullage gas flow rate, we assume that all moisture present in the ullage gas will react with the ternary salt.

The resulting MgOHCl then disassociates into its component ions via reaction (2) to form $MgOH^+$. Given the specifications of the pilot plant and $N_2(g)$, this means that up to 1.8 x 10^{-5} mol H_2O could enter the plant per minute according to equation (3). These results, graphed in Fig. 1, show the potential of accumulation of significant amounts of corrosive $MgOH^+$ over time.

2.3. Mitigation of corrosive impurities in salt

We propose removal of $MgOH^+$ from the ternary salt via an electrochemical purification method, illustrated in Fig. 2. The overall removal of $MgOH^+$ will be accomplished via the net purification reaction (4). To avoid buildup $MgOH^+$ and associated corrosion, rate of this purification process must exceed the rate of impurity formation that was graphed in Fig. 1.

Ongoing laboratory experiments indicate that the electrochemical purification reaction is limited by mass transfer. Specifically, it is limited by diffusion of $MgOH^+$ to the electrode, which is slow. The electrochemical purification reaction at the electrode surface is relatively fast.

Having identified diffusion of $MgOH^+$ as the rate limiting process, we investigated several different geometric configurations for integration of purification unit into the pilot plant to achieve desired purification. First, we considered purification of a small amount of the total flow of molten salt in a loop appended to the main flow, as illustrated in Fig. 3a. Second, we considered use of multiple reactors in parallel, enabling a decrease the volumetric flow rate within each reactor but still purifying all the salt, illustrated in Fig. 3b. Third, we considered use of a single purification cell purifying all the salt, illustrated in Fig 3c.

We evaluated feasibility of each of these approaches by calculation of the electrode surface area required in each case to achieve target purification rate. We selected electrode surface area as a key metric for two reasons: 1) Cost of purification units will scale with electrode surface area. 2) Electrode surface area has previously been identified as a key variable in scaling electrochemical reactors used in industry.(Liu et al. 2014) Thus, the configuration requiring the least surface area will be preferred.

We found that for the pathway depicted in Fig 3a, the flow rate of salt through the purification cell could be lowered, leading to longer residence times. However, since only a fraction of the salt would be purified in this scenario, the purification cell would have to reduce impurity concentration to an extremely low wt. % to achieve

the required purification rate. Our modeling indicated that it would ultimately result in a larger required electrode surface area to purify only part of the salt as compared to purification of all the salt.

For the scenario depicted in Fig. 3b, a lower flow rate is possible in each cell. However, we found that a high Reynolds number and turbulent flow increase mass transport to the electrodes. Thus, for the pilot plant, splitting the salt into multiple parallel purification units adds complexity but does not enhance purification rate.

Ultimately, we found that for the pilot plant, the least surface area would be required for the scenario depicted in Fig. 3c. This also has the advantage of being the simplest design. We note that in a commerical-scale plant with much higher salt flow rate and higher salt volume, similar analysis could yield a different result.

3. Conclusion

Utilizing the specifications of the proposed Gen3 liquid pathway pilot plant, we have calculated a required purification rate for our proposed electrochemical purification method. Furthermore, we have evaluated several different configurations for integration of the purification cell into the pilot plant, and determined that a single purification unit which purifies all of the salt in a single pass is the most viable option for achiving the target purification rate in the Gen3 liquid pathway pilot plant.

4. Tables, figures, equations, and lists

4.1. Figures

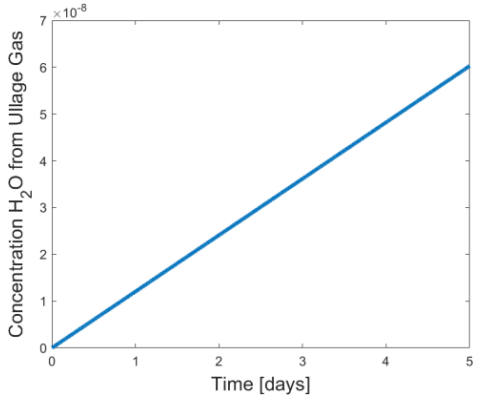

Fig. 1: The concentration of H_2O in the molten salt as it enters from the ullage gas.

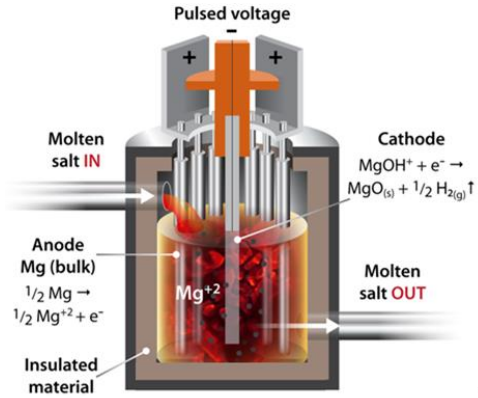

Fig. 2: Illustration of proposed electrochemical purification method. At the cathode, corrosive impurity $MgOH^+$ is electrochemically converted to MgO, a solid which can be removed from salt via filtration. At the anode, dissolution of Mg^+ balances the removal of the Mg in the MgO, keeping the composition of the ternary salt consistent.

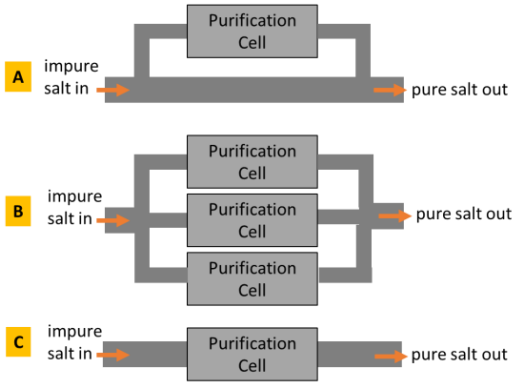

Fig. 3: Possible configuration for molten salt purification using an electrochemical cell. For the pilot plant, our analysis showed that the pathway depicted in 3c required the lowest electrode surface area.

4.2. Equations

$MgCl_2 + H_2O \rightarrow MgOHCl + HCl$
(eq. 1)

$2MgOHCl \rightarrow 2MgOH^+ + 2Cl^-$
(eq. 2)

$$\frac{15\ \text{scf}}{\text{min}} \cdot \frac{1.20\ \text{mol}\ N_2}{1\ \text{scf}} \cdot \frac{1 \times 10^{-6}\ \text{mol}\ H_2O}{1\ \text{mol}\ N_2} = \frac{1.8 \times 10^{-5}\ \text{mols}\ H_2O}{\text{min}}$$
(eq. 3)

$2MgOH^+ + Cl^- + Mg(s) \rightarrow Mg^+ + Cl^- + 2MgO(s) + H_2(g)$
(eq. 4)

5. Acknowledgements

This work was supported by DOE SETO grant CPS #35931 and the Mines/NREL Advanced Energy Systems Graduate Program. We also thank Sridhar Seetharaman, Matthew Earlam, and Stephen James.

6. References

Ding, Wenjin, Judith Gomez-Vidal, Alexander Bonk, and Thomas Bauer. 2019. 'Molten chloride salts for next generation CSP plants: Electrolytical salt purification for reducing corrosive impurity level', *Solar Energy Materials and Solar Cells*, 199: 8-15.

Ding, Wenjin, Hao Shi, Adrian Jianu, Yanlei Xiu, Alexander Bonk, Alfons Weisenburger, and Thomas Bauer. 2019. 'Molten chloride salts for next generation concentrated solar power plants: Mitigation strategies against corrosion of structural materials', *Solar Energy Materials and Solar Cells*, 193: 298-313.

Gomez-Vidal, Judith C., and Robert Tirawat. 2016. 'Corrosion of alloys in a chloride molten salt (NaCl-LiCl) for solar thermal technologies': *Solar Energy Materials and Solar Cells*, 234-44.

Liu, Chenglin, Ze Sun, Guimin Lu, Xingfu Song, Yulong Ding, and Jianguo Yu. 2014. 'Scale-up design of a 300 kA magnesium electrolysis cell based on thermo-electric mathematical models', *The Canadian Journal of Chemical Engineering*, 92: 1197-206.

Mehos, M., Craig Turchi, Judith Vidal, Michael Wagner, Zhiwen Ma, Clifford Ho, William Kolb, Charles Andraka, and Alan Kruizenga. 2017. *Concentrating Solar Power Gen3 Demonstration Roadmap*. OSTI 1338899

Turchi, Craig S., Samuel Gage, Janna Martinek, Sameer Jape, Ken Armijo, Joe Coventry, John Pye, Charles-Alexis Asselineau, Felix Venn, William Logie, Armando Fontalvo, Shuang Wang, Robbie McNaughton, Daniel Potter, Theodore Steinberg, and Geoffrey Will. 2021. "CSP Gen3: Liquid-Phase Pathway to SunShot." OSTI 1807668, United States.

Zhao, Youyang, Noah Klammer, and Judith Vidal. 2019. 'Purification strategy and effect of impurities on corrosivity of dehydrated carnallite for thermal solar applications', *RSC Advances*, 9: 41664-71.